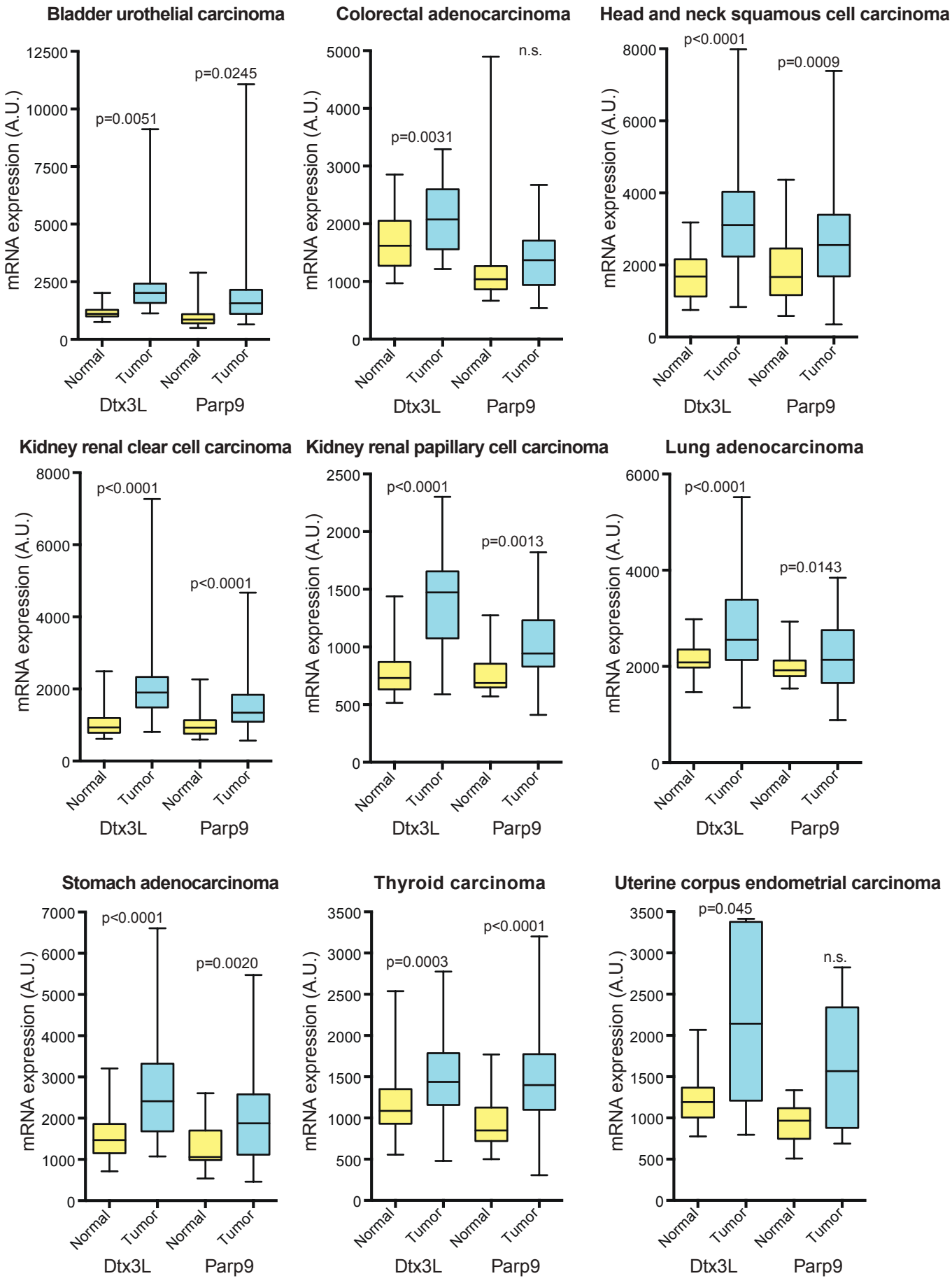

Fig. S1. Related to Fig. 1. Dtx3L and Parp9 expression in TCGA datasets. Box and whisker plots of Dtx3L and Parp9 in cancer (blue) compared to adjacent normal tissue (yellow). Data was downloaded from the publicly available TCGA Data Portal. RNA-Seq by Expectation-Maximization (RSEM) values were used as normalized expression and significance was calculated using a paired *t*-test. Respective sample size for each TCGA Dataset is as follows: BLCA (n=19), COADREAD (n=32), HNSC (n=43), KIRC (n=72), KIRP (n=32), LUAD (n=58), STAD (n=32), THCA (n=59), and UCEC (n=7).

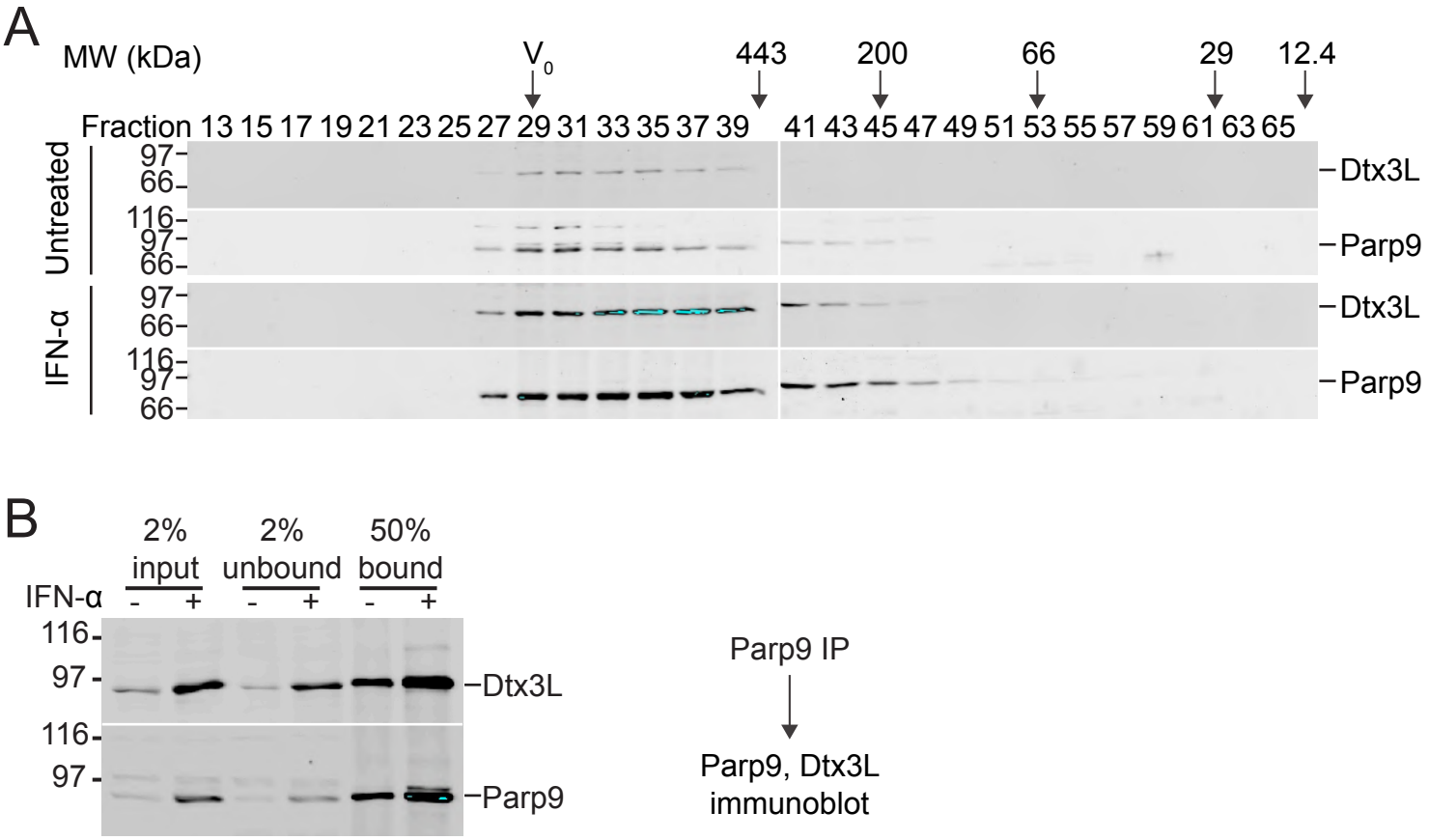

Fig. S2. Related to Fig. 1. Heterodimerization of Dtx3L and Parp9 in prostate cells. (A) Gel filtration chromatography (Superdex 200) showing the apparent molecular sizes of Dtx3L/Parp protein complexes in VCaP prostate cancer cell extracts. Extracts were prepared from VCaP cells that were untreated and treated with IFN-α for 24 hrs. (B) Immunoprecipitation of the Dtx3L/Parp9 complex using an affinity-purified antibody to Parp9.

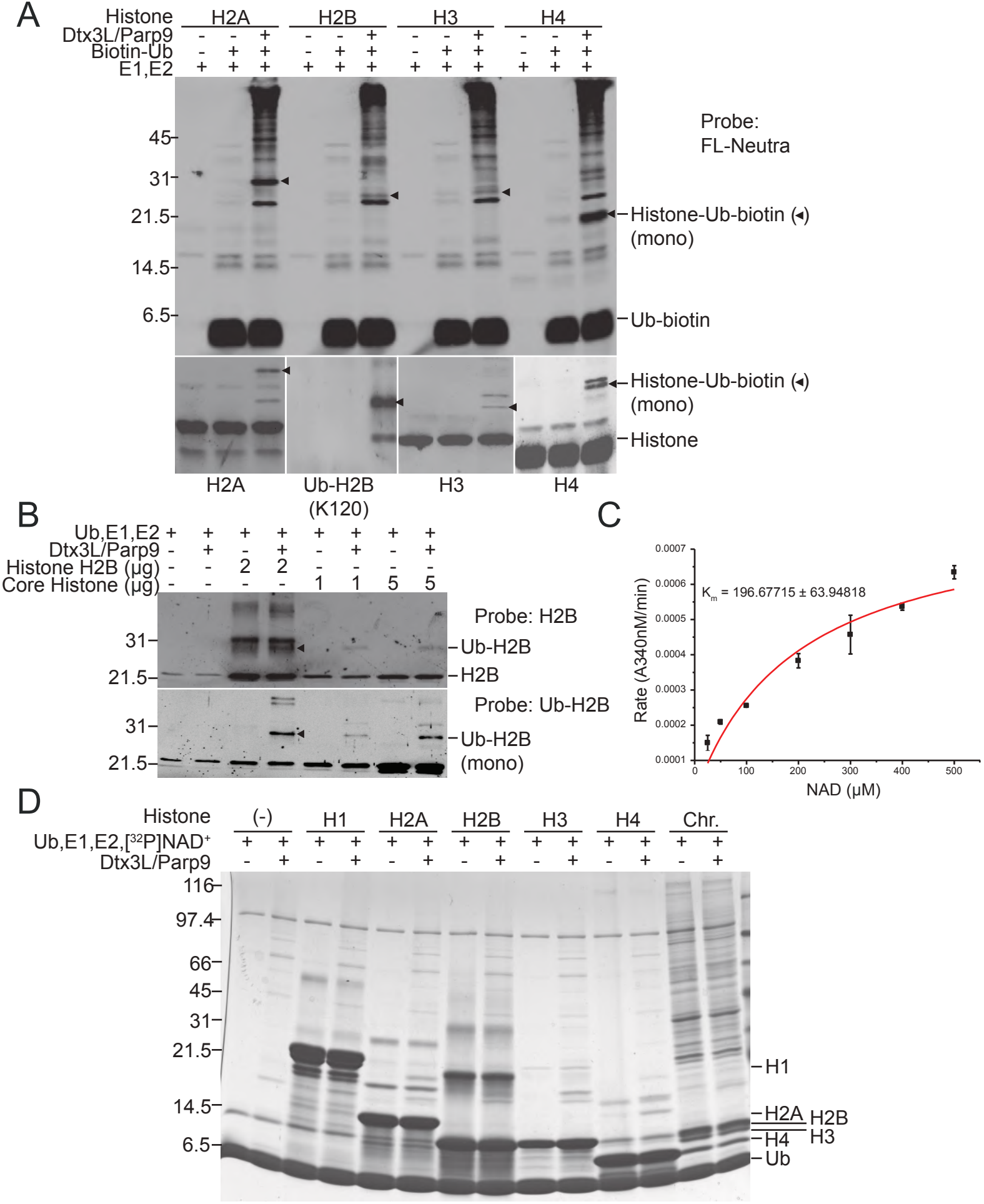

Fig. S3. Related to Fig. 1. Dtx3L/Parp9 contains both Ub E3 ligase and NADase activity. (A) Dtx3L/Parp9- mediated mono-ubiquitylation of Histones H2A, H2B, H3, and H4 assayed using biotin-labeled Ub and detected with Fl-Neutravidin (upper panel). Blots were probed for Histone H2A, Histone H2B-Lys120-Ub, Histone H3, and Histone H4 (lower panel). (B) Dtx3L/Parp9-mediated mono-ubiquitylation of H2B in a core histones preparation from mammalian cells. (C) K_m determination for NAD^+ using a solution assay that measures nicotinamide generated by Dtx3L/Parp9. Data represented as mean ± SD. (D) SDS-PAGE (Coomassie blue) of ADP-ribosylation reactions corresponding to the autoradiograph displayed in **Fig. 1C**.

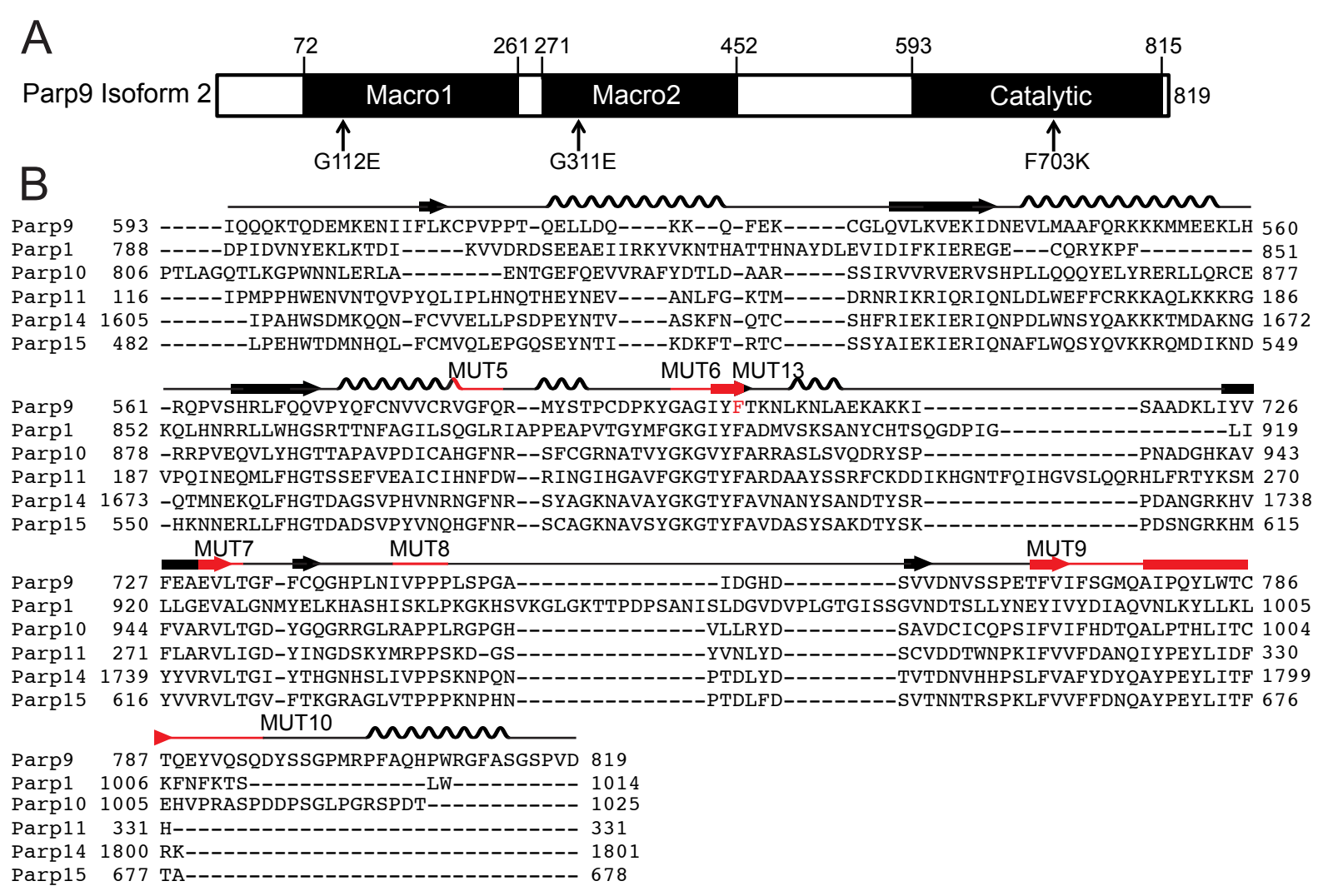

Fig. S4. Related to Fig. 3. Structure-function analysis of Parp9. (A) Domain organization of Parp9 and locations of loss-of-function mutations. (B) Alignment (Clustal-Omega) of Parp catalytic domains. Predicted secondary structure and regions important for heterodimerization with Dtx3L, as well as the F703K mutant are indicated (red). (C, D) Structural models of Parp9 showing the location of small deletions (red) affecting heterodimerization, and the point mutant F703K (red) that selectively reduces ADP-ribosylation of Ub, respectively. The Parp9 catalytic domain model was generated by threading onto the Parp14 structure crystalized with the ligand 3-AB (PDB 3SE2).

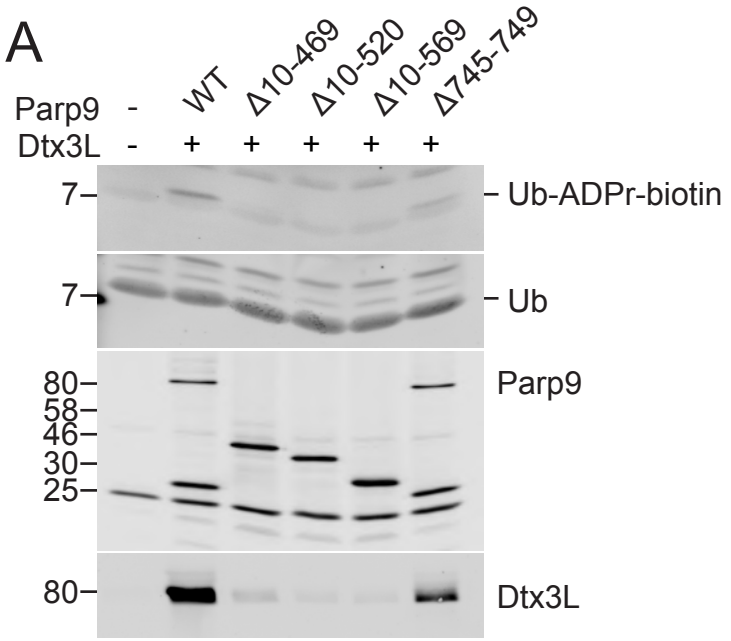

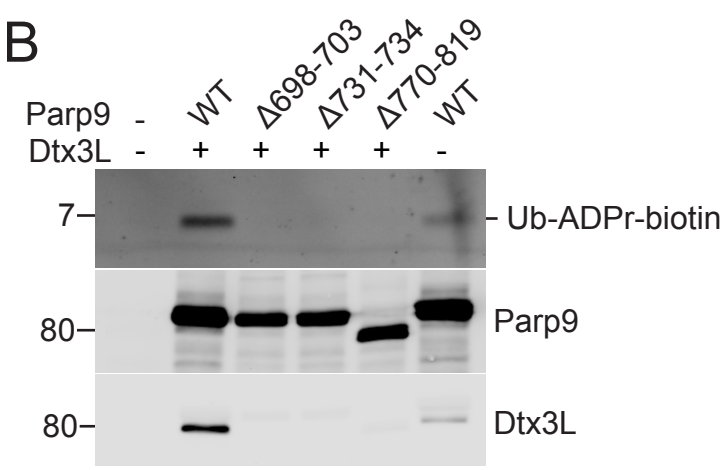

C

Table I. Summary of Parp9 Mutants

Parp9	Description (Parp9 Protein)	% ADP-ribosylation	Dtx3L	% Dtx3L binding
WT	WT	100	Endogenous	100
MUT1	G112, 311E	109	Endogenous	96
MUT2	Δ10-469	2	Endogenous	1
MUT3	Δ10-520	<0.5	Endogenous	1
MUT4	Δ10-569	<0.5	Endogenous	<0.5
MUT5	Δ684-687	1	Endogenous	<0.5
MUT6	Δ698-703	3	Endogenous	1
MUT7	Δ731-734	1	Endogenous	<0.5
MUT8	Δ745-749	56	Endogenous	25
MUT9	Δ770-819	<0.5	Endogenous	<0.5
MUT10	Δ796-819	96	Endogenous	95
WT	WT (*E.coli*)	100	Co-Expression	100
WT	WT (*E.coli*)	0	None	None
MUT11	Y702A (*E.coli*)	145	Co-Expression	87
MUT12	P767A, E768A (E.coli)	94	Co-Expression	230
MUT13	F703K (*E.coli*)	13	Co-Expression	103
MUT1	G112, 311E (*E.coli*)	88	Co-Expression	383

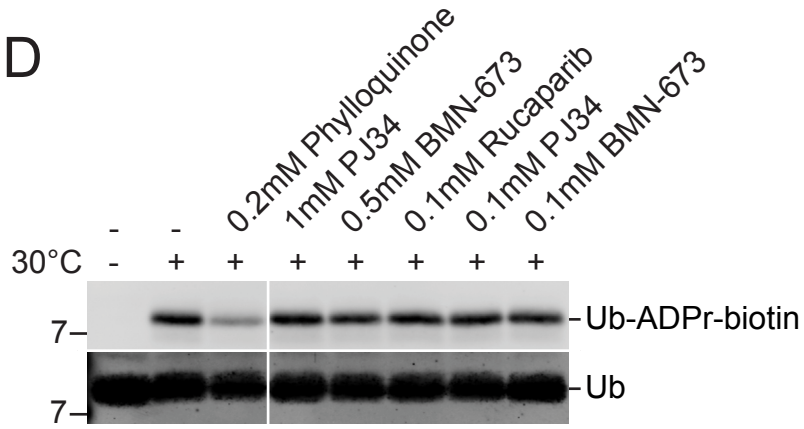

Fig. S5. Related to Fig. 3. Characterization of Parp9 mutants and Parp inhibitors on Ub ADP-ribosylation. (A, B) Analysis of Dtx3L/Parp9 complexes after transfection into 293T cells. The complexes were immunoprecipitated via Parp9 and used in Ub ADP-ribosylation assays. (C) Summary of Parp9 mutants. (D) Effects of Parp inhibitors on ADP-ribosylation of Ub.

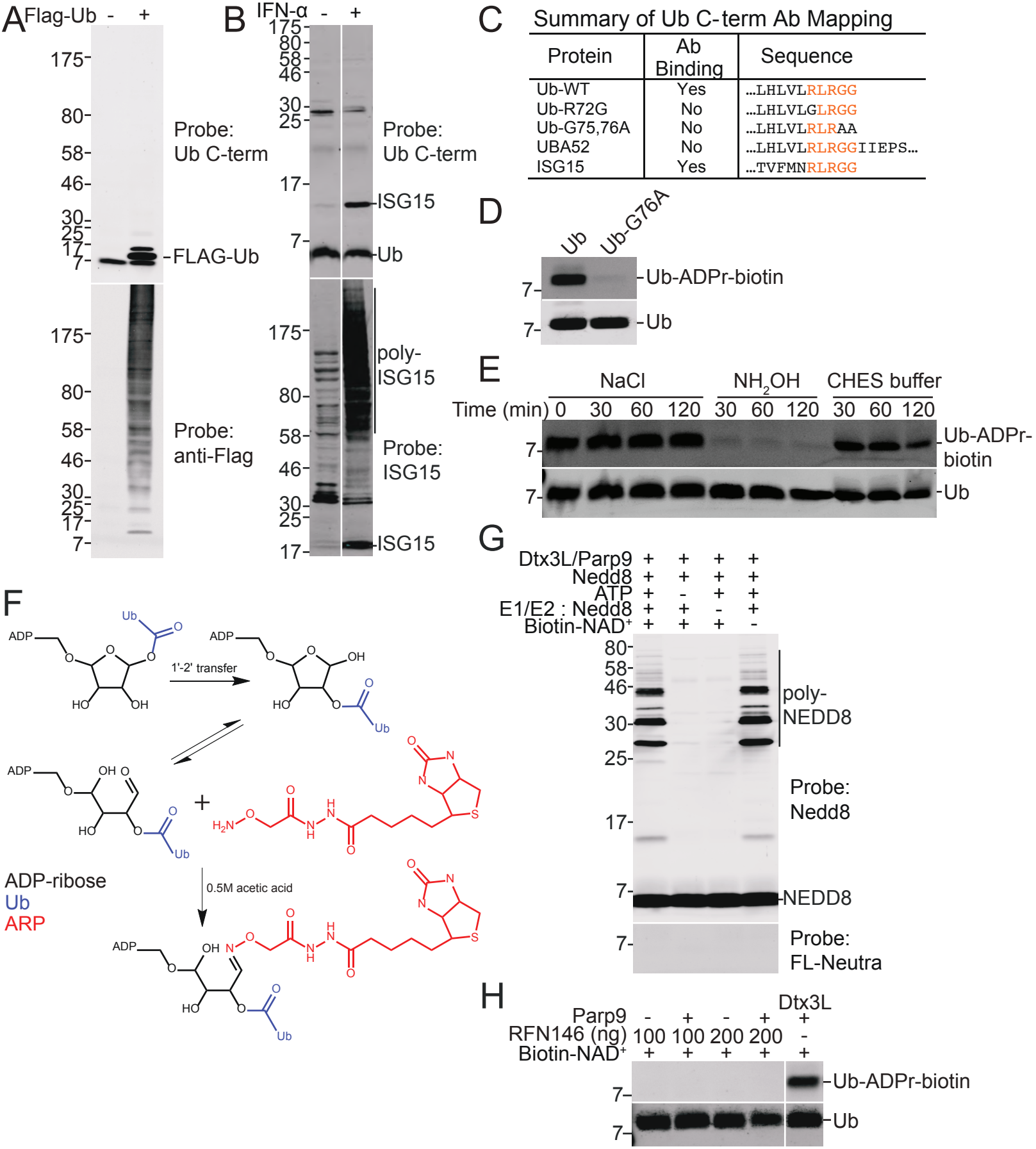

Fig. S6. Related to Fig. 4-6. Characterizing the site of ADP-ribosylation on Ub. (A) Immunoblots of 293T cells transfected with Flag-His-Ub probed with Pan-Ub or Ub C-term antibody. (B) Immunoblots of VCaP cells treated with IFNα (100ng/ml, 24 hrs) probed with ISG15 antibody or Ub C-term antibody. (C) Alignment of the C-terminal regions of Ub proteins probed in this study. UBA52 is a precursor form of Ub. The deduced epitope for the antibody is shown in orange. (D) Mutation of Ub G76A abolishes ADP-ribosylation of the C-terminus. (E) Treatment of Ub-ADPr with NH_2OH, NaCl, and CHES. (F) Proposed reaction scheme for ARP modification of Ub-ADPr. (G) ADP-ribosylation assay using the Ub-related protein Nedd8. (H) ADP-ribosylation assay using the E3 RNF146.

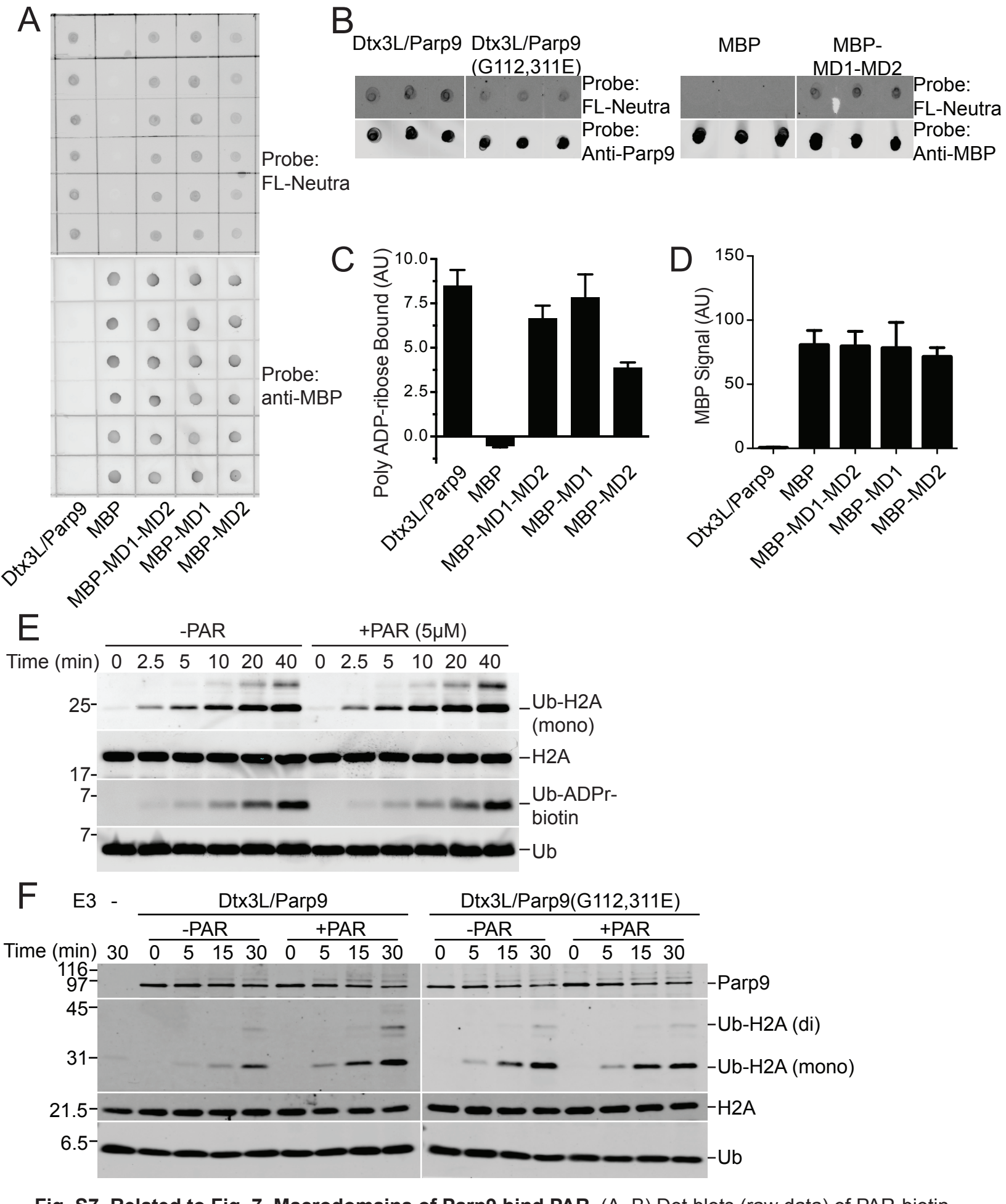

Fig. S7. Related to Fig. 7. Macrodomains of Parp9 bind PAR. (A, B) Dot blots (raw data) of PAR-biotin binding to Dtx3L/Parp9. (C) Quantification of PAR-biotin binding normalized to MBP. Data represented as mean and SD. (D) Quantification of MBP binding. (E) PAR effect on E3 activity. (F) PAR effect on E3 activity of the Dtx3L/Parp9 heterodimer (WT and macrodomain mutants).